Use of the Connectivity Modeling System to estimate movements of red snapper (*Lutjanus campechanus*) recruits in the northern Gulf of Mexico

M. Karnauskas, J. F. Walter III, and C. B. Paris

SEDAR52-WP-20

27 November 2017

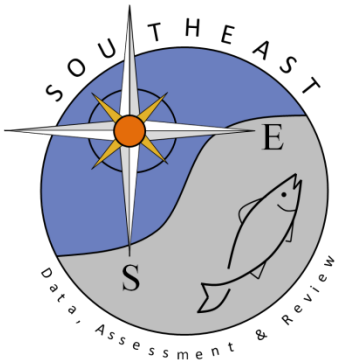

Please cite this document as:

Karnauskas, M., J. F. Walter III, and C. B. Paris. 2017. Use of the Connectivity Modeling System to estimate movements of red snapper (*Lutjanus campechanus*) recruits in the northern Gulf of Mexico. SEDAR52-WP-20. SEDAR, North Charleston, SC. 13 pp.

SEDAR52-AWXX

Use of the Connectivity Modeling System to estimate movements of red snapper (*Lutjanus campechanus*) recruits in the northern Gulf of Mexico

M. Karnauskas[1], J. F. Walter III[1], and C. B. Paris[2]

[1]Southeast Fisheries Science Center

Sustainable Fisheries Division

75 Virginia Beach Drive

Miami, FL 33149

[2]University of Miami

Rosenstiel School of Marine and Atmospheric Science

Division of Applied Marine Physics

4600 Rickenbacker Causeway

Miami, FL 33149

****

Introduction

This research makes use of a biophysical modeling framework to understand recruitment dynamics of the red snapper (*Lutjanus campechanus*) in space and time. The purpose of this research is twofold: 1) to understand the locations of larval sources and sinks within the Gulf of Mexico, and 2) to predict recruitment strength of red snapper due to the effects of oceanographic currents on an annual basis. This annual index of recruitment deviations expected from oceanographic factors can be used to inform recruitment patterns in the stock assessment model. We use the Connectivity Modeling System (Paris et al. 2013), an individual-based model which estimates the movement of particles in a 3-D velocity field, and has the capacity to simulate complex behaviors such as those displayed by fish larvae. The connectivity model is used to simulate the release of red snapper eggs during the spawning season for years 2003 – 2017.

This paper is an update of a working paper that was produced for SEDAR 31 (Karnauskas et al. 2013). Since the publication of the original document, a number of improvements have been made to both the modeling framework and the data inputs. The Connectivity Modeling System has undergone additional testing and development. The biological inputs have been updated with new data, as available. Finally, additional sensitivity analyses have been carried out and the outputs have been refined for clarity.

Methods

Connectivity Modeling System

The Connectivity Modeling System (CMS) is a biophysical modeling system based on a Lagrangian framework, and was developed to study complex larval migrations (Paris et al. 2013). The CMS uses outputs from hydrodynamic models and tracks the three-dimensional movements of advected particles through time, given a specified set of release points and particle behaviors. Optional modules are provided to allow for complex behaviors and movements, simulating observed biological phenomena such as egg buoyancy, ontogenetic vertical migration, and tidal stream transport. The specific model set up used for this study is outlined in detail below.

Ocean velocity fields

The hydrodynamic model we used was the HYCOM + NCODA Gulf of Mexico 1/25° Analysis, a freely available ocean model with daily velocity fields available from 2003 – present (www.hycom.org). HYCOM is a hybrid isopycnal coordinate ocean model (i.e., isopycnal in the stratified open ocean, fixed-depth in the unstratified surface layers, and terrain-following in shallow coastal waters), while allows for optimal simulation of both coastal and open-ocean features simultaneously (Chassignet et al. 2007). The model is data-assimilative, using real-time observations of the ocean's surface via satellite altimetry, as well as vertical profile information from CTDs, the ARGO observation program, and other sources. This allows for a three-dimensional depiction of ocean currents in real time at a relatively high resolution. At the time of this publication, four different experiments were available for the Gulf of Mexico 1/25° Analysis: experiment 20.1 (covering the period Jan 2003 – July 2010), experiment 30.1 (June

2010 – Mar 2012), experiment 31.0 (Apr 2009 – Jul 2014) and experiment 32.5 (Apr 2014 – Nov 2017). For the years that had coverage by multiple experiments (2009, 2010, 2011, and 2014) we carried out sensitivity analyses to understand the effect of the hydrodynamic field forcing on the resulting estimates of recruitment strength.

Initial conditions of the biological model

Spawning time

Spawning season for red snapper in the northern GOM generally begins in May and ends in early fall (Collins et al. 2011, Rooker et al. 2004) and thus we simulated spawning activity throughout the peak spawning period of May 1 to August 31 every year. Spawning is estimated to occur approximately every 3 days (Brown-Peterson et al. 2008; Jackson, et al. 2006; Woods 2003) and there is no lunar periodicity apparent in the timing of spawning (Jackson et al. 2006); we simulated particle releases every 3 days throughout the spawning period for all years. To account for the fact that the average spawning fraction varies throughout the spawning season, we scaled the spawning releases by a reported statistical relationship relating the proportion of red snapper females bearing spawning markers with time of year (Porch et al. 2015).

Spawning location

We based the location of egg releases on a probabilistic model of red snapper biomass across space (Karnauskas et al. 2017). The analysis included surveys of artificial structures (e.g., oil rigs and artificial reefs) and thus accounts for spawning from these locations. Because the model is age-structured, and the fecundity at age has been estimated, the distribution map is calculated in terms of expected number of eggs released over the spatial domain. This map then forms the basis of the locations of the simulated egg releases, with numbers of eggs scaled to the relative predicted density. Red snapper have been observed to spawn at depths of 40-45 m in the GOM (P. Bennett, pers. comm.). In the South Atlantic, active spawners (i.e., fish with fresh postovulatory follicles, estimated to be within 2 hours of spawning) were collected from depths of 15-73m (Lowerre-Barbieri et al. 2015). Therefore, the depth of particle release was parameterized as follows: particles were released at 45m for depths greater or equal to 50m, at 2m above the bottom for depths between 15 m and 50 m, and no releases were performed in shallow depths < 15m.

Egg buoyancy and vertical migration

In the CMS, vertical movements are defined via a probability matrix, which specifies the distribution of virtual larvae in the water column throughout time. Time steps for the probability matrix are most logically defined by using different stages of larval metamorphosis (e.g., hatching, preflexion, postflexion), as larvae tend to shift in their vertical distributions with these changes. Red snapper eggs are reported to hatch at approximately 24 hours after fertilization (Rooker et al. 2004), and Drass et al. (2000) reported that notochord flexion began at 12 days after hatching and was complete by 15 days after hatching. We therefore defined the following phases (in days after release): hatching 0-1 days, preflexion 2-12 days, flexion 13-16 days, and postflexion 17-25 days.

To parameterize the vertical distributions of eggs, we used a detailed study of lutjanid movements based on a comprehensive depth-stratified survey in the Florida Straits (D'Alessandro et al. 2010). This study was comprehensive in coverage in both space and time, and sampled depths to 100m, but reported capture of only two individual red snappers. However, sample sizes of a number of different congeners was high (>100), and results showed that the distribution of lutjanid larvae did not vary greatly among species (D'Alessandro et al. 2010). Because vertical larval distributions have a large influence on the results, and because this was considered the greatest area of uncertainty regarding the reproductive and larval biology of red snapper, we carried out a series of sensitivity runs to quantify the effect of this uncertainty on the estimates. From D'Alessandro et al. (2010), we selected three congeners with high sample sizes and similar life history to red snapper (gray snapper *L. griseius*, lane snapper *L. synagris*, mutton snapper *L. analis*) and parameterized the vertical distributions according to observations for these three species. Mutton snapper was thought to be the most closely related to red snapper based on the depth range of adults and maximum body length, and was used as a "base case" for further sensitivity runs.

Little has been published on the egg properties of red snapper, and thus we used depth-stratified sampling observations of eggs in the Gulf of Mexico to inform the vertical distributions of eggs. To inform these distributions we used a survey of three sites off the coast of Alabama, sampled at 11 days between May and September (F. Hernandez, pers. comm). Maximum depths sampled at the three sites were 18m, 30m, and 60m; most spawning activity is estimated to occur at depths greater than 18m, so we considered only the deeper two sites to be potentially representative of average egg distributions. We used the observed distributions of egg numbers by depth at each site in separate sensitivity runs. Additionally, because the distribution at the 60m site was dominated by a single outlier where the egg concentration was an order of magnitude higher than all other sites, we carried out a sensitivity run excluding the outlier. Because the distributions varied significantly between the two sites (average depths of eggs at the two sites were 3m and 30m respectively), we considered that there was substantial uncertainty in egg distributions, and used a simple uniform distribution from spawning depth to surface as the base case for comparison.

The sensitivity runs carried out were as follows. For each case, the model parameters were changed as described, the simulation run, and outputs summarized.

1. Vertical movements parameterized according to mutton snapper (*L. analis*) distributions; egg movements parameterized as a uniform distribution
2. Vertical movements parameterized according to mutton snapper (*L. analis*) distributions; egg movements parameterized according to deep AL shelf site observed distributions
3. Vertical movements parameterized according to mutton snapper (*L. analis*) distributions; egg movements parameterized according to deep AL shelf site observed distributions after removing outlier
4. Vertical movements parameterized according to mutton snapper (*L. analis*) distributions; egg movements parameterized according to shallow AL shelf site observed distributions
5. Vertical movements parameterized according to lane snapper (*L. synagris*) distributions; egg movements parameterized as a uniform distribution

6. Vertical movements parameterized according to gray snapper (*L. griseus*) distributions; egg movements parameterized as a uniform distribution

Additionally, to understand the effect of HYCOM experiment we tested the base case (#1) with alternative experiments available for certain years.

7. Vertical movements parameterized according to mutton snapper (*L. analis*) distributions; egg movements parameterized as a uniform distribution, with alternative hydrodynamic forcing for years 2009 (expt 20.1), 2010 (expts 20.1 & 30.1), 2011 (expt 30.1), and 2014 (expt 31.0).

Settlement

Red snapper begin settling out of the pelagic stage no earlier than 26 days, with most settling by 28 days of age, and maximum settlement age is estimated to be about 30 d (Szedlmayer & Conti 1999; Drass et al. 2000; Rooker et al. 2004). We therefore specified the settlement competency period as lasting for 5 days (26-30 d). High-value settlement habitat is estimated to occur between 15 and 64 m depth (Johnson et al. 2013). Using the global 30 arc-second bathymetry data grid available from GEBCO (General Bathymetric Chart of the Oceans; www.gebco.net), we extracted contours at the 15 m and 64 m isobaths for the northern GOM. Suitable settlement habitat was defined by the area between these isobaths. Successful settlement is defined by those particles which reach the suitable settlement habitat during the competency window, given the suite of previously described parameterized behaviors and attributes.

Other CMS modules

We used the turbulence module of CMS, which adds a random component to the motion of the particles to represent turbulent diffusion. This component represents sub-grid turbulent processes unresolved by the hydrodynamic model grid size. We used a value of 15 $m^2 s^{-1}$ for horizontal diffusivity and 10^{-4} $m^2 s^{-1}$ for vertical diffusivity. We also used the 'avoid coast' module of CMS, which prevent particles from getting stranded on the land mask. Because fish larvae are not passive drifters, they can likely swim away from the coast to avoid being stranded. This module thus provides a more realistic estimate of the movements of fish larvae near coasts. Additionally, CMS provides an algorithm for putting particles back in the ocean if they are transported through the uppermost depth level, which was used in this simulation.

Results

The results presented here are based on simulations where the total number of particles released was kept constant across months and across years. This allows us to consider changes in recruitment patterns due exclusively to annual variation in ocean current patterns, and not related to changes in spawning stock biomass. The index can thus be considered as representative of annual recruitment deviations, prior to any density-dependent processes occurring after settlement out of the pelagic environment.

Relative recruitment strength across the entire northern GoM varied across years, with the greatest number of successful recruits occurring in 2012 (Fig. 1). The most recent period (2014 – 2017) was estimated to have recruitment below the overall average for the study period. Trends over time were similar across the different sensitivity runs, although the variability in recruitment strength differed among runs (Fig. 2). Notably, sensitivity run #6, which was based on vertical movements of larval gray snapper, had higher year-to-year variability. Varying assumptions about the egg distributions had some influence on the year-to-year trends, but the largest differences were seen among runs where vertical distributions at the preflexion and postflexion stages were varied.

For most years, the use of alternative hydrodynamic model experiments in forcing the model did not have a large influence on results; estimates of recruitment were similar regardless of forcing. The exception to this was for the year 2014 – using the 31.0 experimental forcing gave a much higher estimate of recruitment strength than using experiment 32.5 (Fig. 2).

Because the last year of recruitment estimated (2017) was estimated to be the lowest in the series, we created additional figures to understand the mechanisms driving this trend. The largest decrease in recruitment relative to other years occurred in June 2017, and we plotted the June trajectories for comparison with other years. Figure 3 shows the terminal locations of particles representing larvae (those successfully settled, or advected offshore) for the two highest and lowest years of recruitment as estimated by the model. The reduced recruitment in 2017 is driven by increased offshore advection of larvae which prevented settlement activity within the specified competency period (Fig. 4).

While the recruitment index represents dynamics of the entire northern Gulf red snapper population, model output at the coordinate level also allows summarization of results at finer spatial scales. These spatial dynamics are easily viewed in the form of a connectivity matrix which shows the spatial patterns in source and sinks for larvae that have successfully settled (Fig. 5). In general, self-recruitment of larvae occurs; i.e., larvae settle at locations in close geographical proximity to the location at which they were spawned. While the spatial patterns in transport can vary quite dramatically across small scales, on average for the period 2003 – 2017, there is a tendency for larvae to settle in adjacent areas slightly eastward. In other words, a given area tends to supply its neighboring areas to the east to a greater extent than it supplies its neighbors to the west. The numbers connectivity matrix can also be summed up according to relevant management levels such as state boundaries (Fig. 6). Texas and Florida are highly self-recruiting – approximately 90% of larvae settling are estimated to originate from those states. Louisiana is estimated to receive roughly half of its larvae from local waters and just under half of its larvae from Texas. Alabama and Mississippi are estimated to receive substantial input from all states. Mississippi is unique in that it is estimated to receive only a small percent larvae originating from local waters; Louisiana and Alabama appear to be important suppliers of larvae to Mississippi state waters. Standard errors around these estimates from the sensitivity runs are relatively small, indicating that results are robust to variation in model inputs, at least for the range of sensitivity analyses explored in this study.

Discussion

This paper represents an update of SEDAR31-AW10; the present working paper adds an additional five years of recruitment estimates and includes additional refinements in model parameterizations. These refinements include a better characterization of spawning season and spawning location based on two recent peer-reviewed publications, updates to vertical migration behavior of larvae with new data sources, and more robust characterization of uncertainty with respect to egg distributions, vertical migration of larvae, and hydrodynamic forcing. As new data become available, model parameterizations can continue to be refined.

Some caution should be taken in interpreting trends during the last four years (2014 – 2017) relative to earlier years of the simulation, due to the lack of overlap in hydrodynamic experiments. Results for the year 2014 based on an older experiment (expt 31.0) yielded higher recruitment estimates than those based on the newer expt 32.5. Unfortunately there are no other years for comparison of these two particular experiments, which leaves some question as to whether this phenomenon is simply an outlier, or whether the expt 32.5 tends to yield a negative bias in the recruitment index. Differences in the hydrodynamic experiments include the introduction of tidal forcing in expt 32.5 and an increase in the number of vertical layers from 20 to 27. Further investigation is needed to understand the effect of particular hydrodynamic experiment on the simulation of recruitment mechanisms. An inspection of model outputs such as the average depth distributions and average longitudinal and latitudinal position of larvae did not reveal any systematic bias in the most recent experiment.

Taking the last four years into consideration independently, recruitment strength in year 2017 was estimated to be well below average. Inspection of the individual particle trajectories shows that many larvae were advected further offshore relative to other years. This is due to the influence of the Loop Current, which varies in the extent of its northward intrusion from year to year (Lindo et al. 2012).

Acknowledgements

We thank F. Hernandez, E. D'Alessandro, G. Zapfe and D. Hanisko for their assistance with data on red snapper larval and egg distributions. We acknowledge A. Vaz for programming support. We thank S. Cass-Calay, S. Sagarese, K. Shertzer, N. Kilbansky and D. Goethel for their helpful comments on this research.

References

Brown-Peterson, N.J., K.M. Burns and R.M. Overstreet. 2008. Regional Differences in Florida Red Snapper Reproduction. Faculty Publications from the Harold W. Manter Laboratory of Parasitology. Paper 438.

Chassignet, E.P, H.E. Hurlburt, O. M. Smedstad, G.R. Halliwell, P.J. Hogan, A.J. Wallcraft, R. Baraille and R. Bleck. 2007. The HYCOM (HYbrid Coordinate Ocean Model) data assimilative system. Journal of Marine Systems 65:60- 83

Collins, L.A., G.R. Fitzhugh, L. Mourand, L.A. Lombardi, W.T. Walling, Jr., W.A. Fable, M.R. Burnett, and R.J. Allman. 2001. Preliminary results from a continuing study of spawning and

fecundity in the red snapper (Lutjanidae: *Lutjanus campechanus*) from the Gulf of Mexico, 1998-1999. Proceedings of the 52nd Annual Gulf and Caribbean Fisheries Institute 52:34-47.

D'Alessandro, E.K., S. Sponaugle and J.E. Serafy. 2010. Larval ecology of a suite of snappers (family: Lutjanidae) in the Straits of Florida, western Atlantic Ocean. Marine Ecology Progress Series 410:159-175.

Drass, D. M., K. L. Bootes, J. Lyczkowski-Shultz, B. H. Comyns, G. H. Holt, C. M. Riley, and R. P. Phelps. 2000. Larval development of red snapper *Lutjanus campechanus*, and comparisons with co-occurring snapper species. U.S. National Marine Fisheries Service Fishery Bulletin 98(3):507–527.

Jackson, M. W., D. L. Nieland and J.H.J. Cowan. 2006. Diel spawning periodicity of red snapper Lutjanus campechanus in the northern Gulf of Mexico. Journal of Fish Biology 68:695–706.

Johnson, D.W., H.M. Perry and J. Lyczkowski-Shultz. 2012. Connections between Campeche Bank and Red Snapper Populations in the Gulf of Mexico via modeled larval transport. SEDAR31-RD45. SEDAR, North Charleston, SC. 31 pp.

Karnauskas, M., J.F. Walter, and C.B. Paris. 2013. Use of the Connectivity Modeling System to estimate movements of red snapper (*Lutjanus campechanus*) recruits in the northern Gulf of Mexico. SEDAR31-AW10. SEDAR, North Charleston, SC. 20 pp.

Karnauskas, M., J.F. Walter III, M.D. Campbell, A.G. Pollack, J.M. Drymon and S. Powers. 2017. Red snapper distribution on natural habitats and artificial structures in the Northern Gulf of Mexico, Marine and Coastal Fisheries 9(1): 50-67.

Lindo-Atichati, D., F. Bringas, G. Goni, B. Muhling, F.E. Muller-Karger and S. Habtes. 2012. Varying mesoscale structures influence larval fish distribution in the northern Gulf of Mexico. Marine Ecology Progress Series 463:245-257.

Lowerre-Barbieri, S., L. Crabtree, T. Switzer, S.W. Burnsed and C. Guenther. 2015. Assessing reproductive resilience: an example with South Atlantic red snapper *Lutjanus campechanus*. Marine Ecology Progress Series 526:125–141.

Paris, C.B, J. Helgers, E. Von Sebille and A. Srinivasan. 2013. Connectivity Modeling System: a probabilistic modeling tool for the multi-scale tracking of biotic and abiotic variability in the ocean. Environ. Modelling and Software. 42:47-54.

Porch, C.E., G.R Fitzhugh and B.C. Linton. 2013. Modeling the dependence of batch fecundity and spawning frequency on size and age for use in stock assessments of red snapper in U.S. Gulf of Mexico waters. SEDAR31-AW03. SEDAR, North Charleston, SC. 22 pp.

Rooker, J. R., A. M. Landry, B. W. Geary, and J. A. Harper. 2004. Assessment of a bathymetric high and associated habitats as nursery grounds of postsettlement red snapper. Estuarine, Coastal, and Shelf Science 59:653–661.

Szedlmayer, S.T., and J. Conti. 1999. Nursery habitats, growth rates, and seasonality of age-0 red snapper, Lutjanus campechanus, in the northeast Gulf of Mexico. Fisheries Bulletin 97:626-635.

Woods, M.K. 2003. Demographic differences in reproductive biology of female red snapper (*Lutjanus campechanus*) in the northern Gulf of Mexico. Thesis. Department of Marine Sciences, University of South Alabama, Dauphin Island, Alabama. 128 pages.

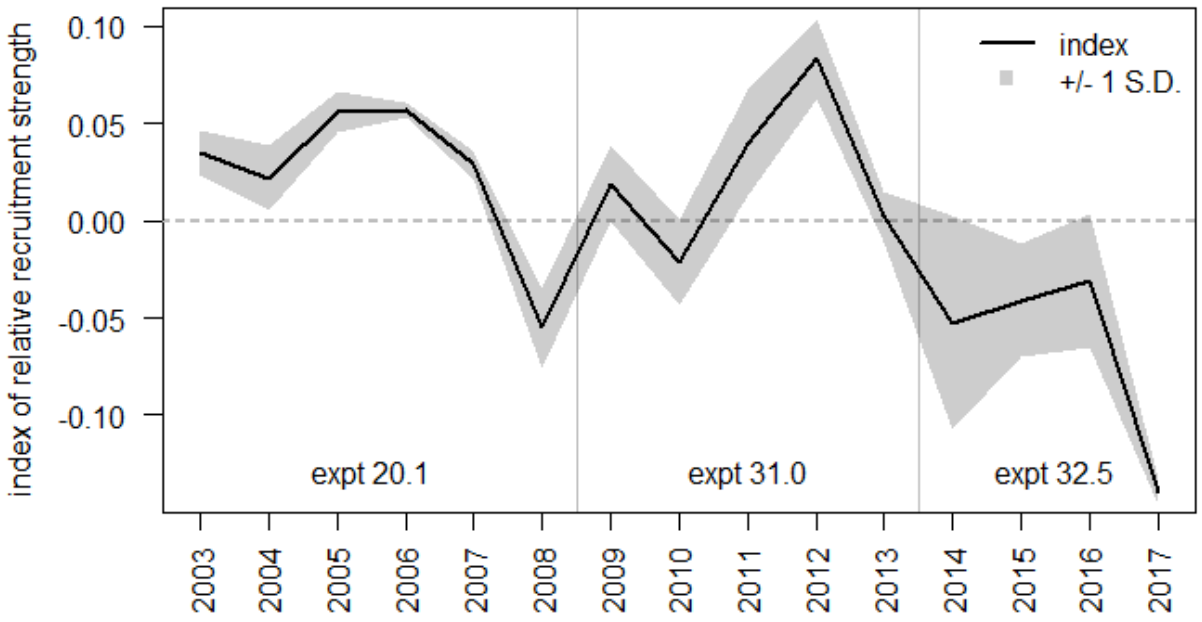

Figure 1. Index of expected annual recruitment strength for northern Gulf of Mexico red snapper with standard deviation. Time periods covered by the different HYCOM hydrodynamic experiments used in the base run are denoted by vertical lines.

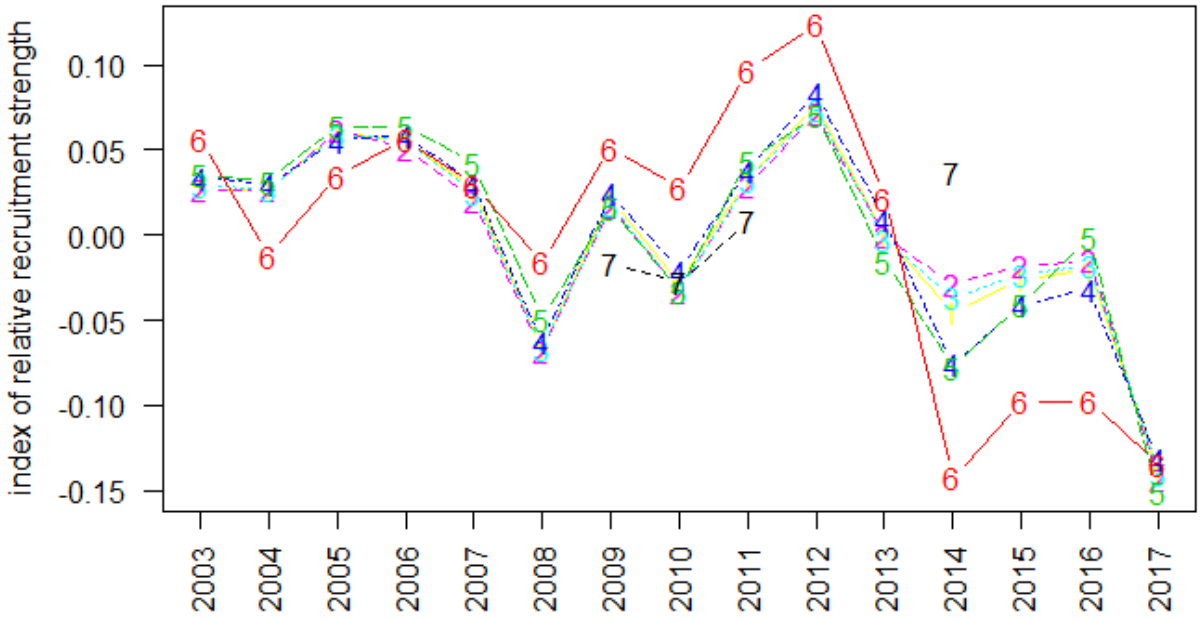

Figure 2 Index of expected recruitment strength for northern Gulf of Mexico red snapper as estimated by the individual sensitivity runs. Numbers refer to model runs listed in the methods.

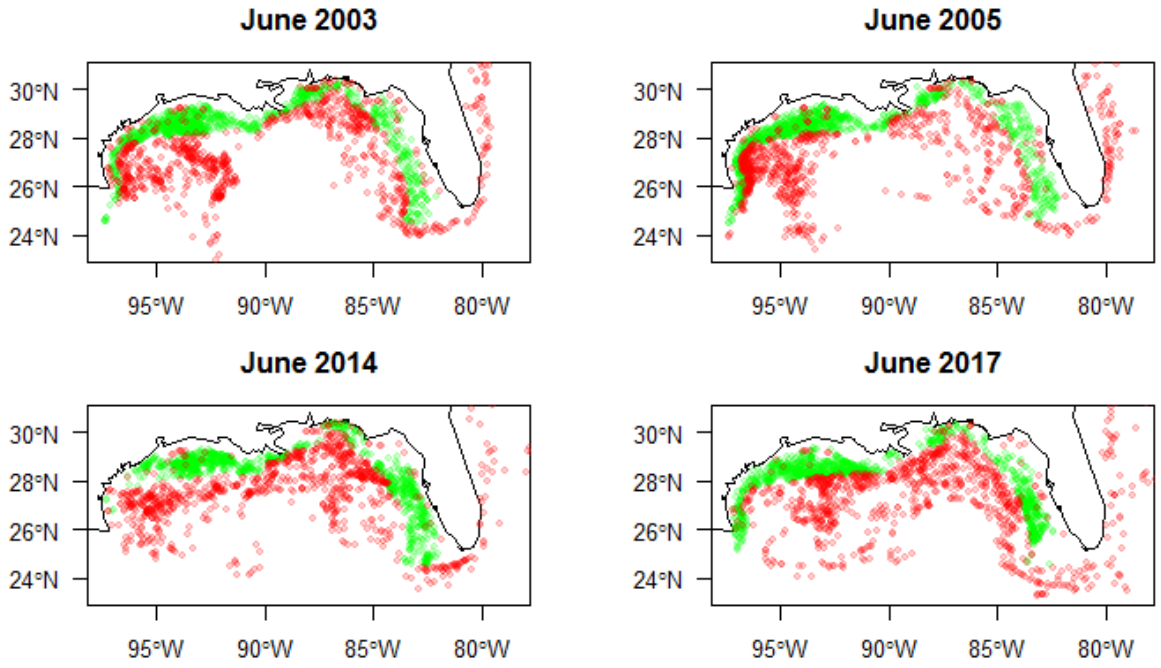

Figure 3. Comparison of transport for two months with highest estimated recruitment success (June 2003 and 2005, top) and two months with lowest estimated recruitment success (June 2014 and 2017, bottom). Green circles denote settlement locations of successfully recruiting particles. Red circles denote ending location of particles that did not successfully settle at the end of the 30-day simulation.

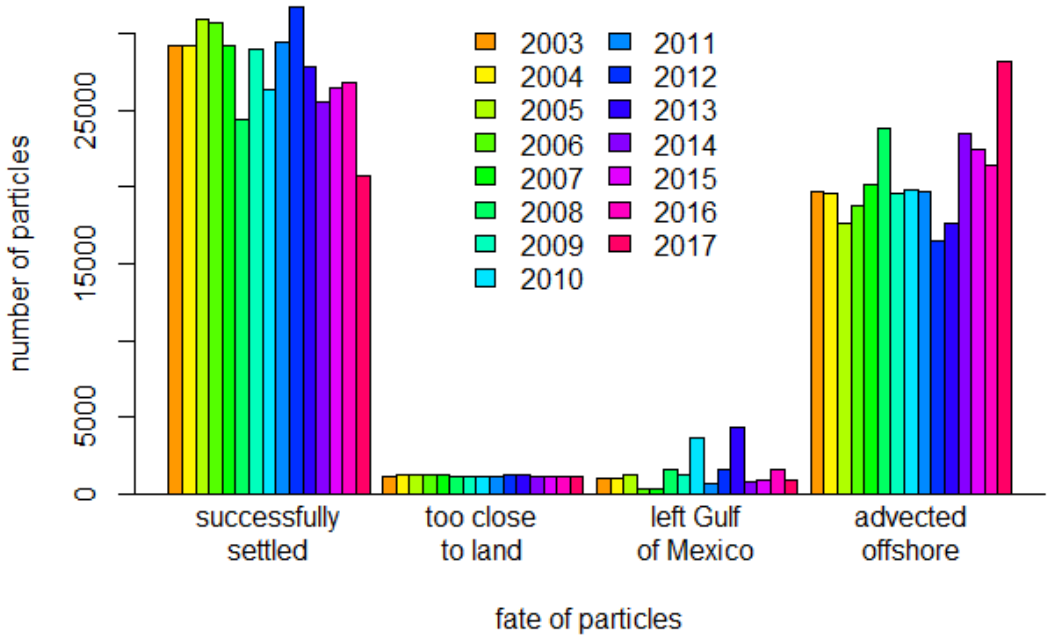

Figure 4. Barplot showing numbers of particles with different fates at the end of the simulation.

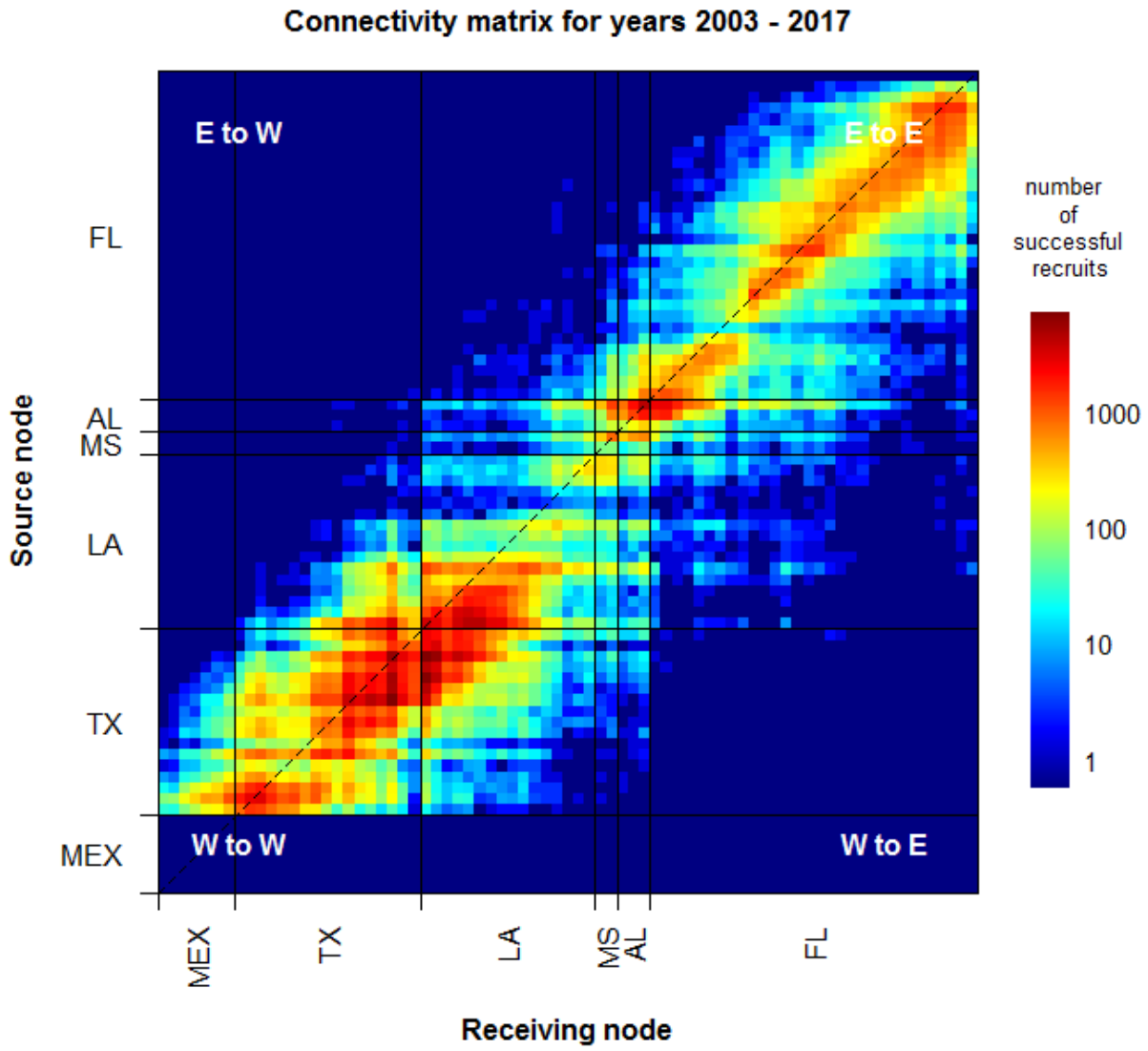

Figure 5. Connectivity matrix for the base model run, averaged across all years. Rows are source nodes (particle release sites) and columns are receiving nodes (particle settlement sites); nodes are ordered clockwise from Mexico to Florida. Self-recruitment is indicated by the dashed diagonal line. Solid lines denote state water boundaries.

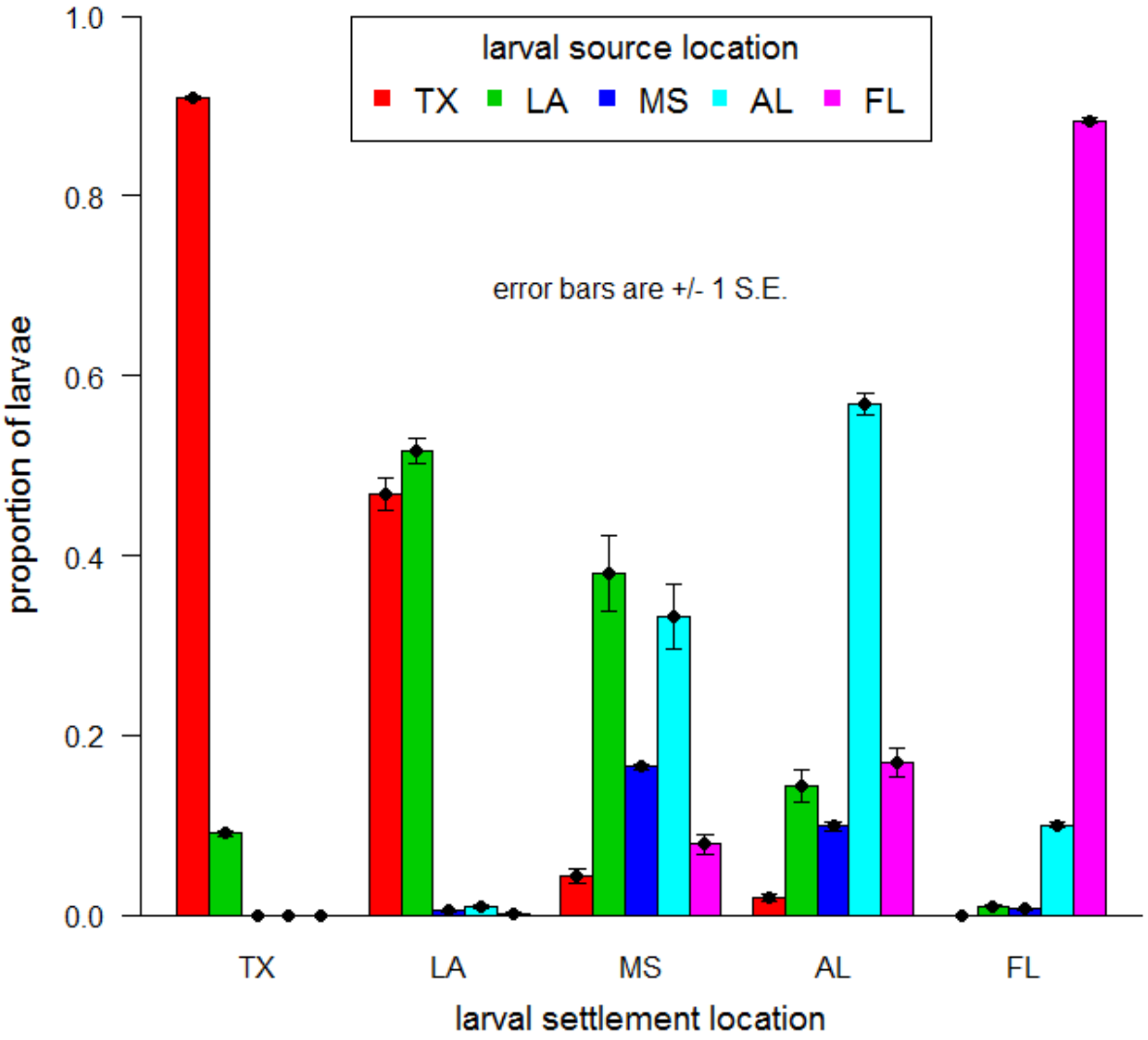

Figure 6. Larval connectivity estimates summed up at the state boundary level. Barplot denotes proportion of the larvae successfully settling in each state that originated from each of the respective states. Standard errors pertain to uncertainty surrounding different sensitivity runs.